JOURNAL OF Materials CHEMISTRY

Hydrothermal synthesis and structural characterization of a new layered zincophosphate co-templated by diprotonated 1,6-diaminohexane and orthoboric acid molecules†

Michael Wiebcke*

Universität Konstanz, Fachbereich Chemie, D-78457 Konstanz, Germany. E-mail: michael.wiebcke@uni-konstanz.de

Received 8th June 2001, Accepted 17th October 2001
First published as an Advance Article on the web 21st November 2001

The zincophosphate $[Zn_3(PO_4)_2(HPO_4)]\cdot H_3N(CH_2)_6NH_3\cdot H_3BO_3$, **I**, has been synthesized by mild hydrothermal methods, and the crystal structure determined by single-crystal X-ray diffraction. In the structure, corner-linked ZnO_4, PO_4 and $PO_3(OH)$ tetrahedra form anionic layers that contain 3-, 4-, 5- and 8-membered rings and may be considered constructed from columns of Zn_5P_4 cage-like building units. The layers are interleaved by composite layers of diprotonated 1,6-diaminohexane and boric acid molecules. The acid molecules stabilize a bilayer-like arrangement of the organic dications. The templates interact with the zincophosphate layers by N–H···O and O–H···O hydrogen bonds. According to thermogravimetry, variable-temperature powder X-ray diffraction and FT-IR spectroscopy studies, **I** transforms at 478 K into another crystalline layered zincophosphate with release of one water molecule per formula unit originating from condensation between terminal P–OH groups and boric acid molecules. The crystallinity disappears at *ca.* 600 K.

Introduction

Two-dimensional (2D) layered and three-dimensional (3D) open-framework inorganic materials are of considerable interest due to their established or potential applications in sorption and separation, heterogeneous catalysis, ion-exchange and as advanced host–guest systems. Meanwhile, a broad range of compositions of these materials is known.[1] Since the first reports of open-framework zincophosphates with zeolite-like structures by Stucky and coworkers,[2] numerous materials with a rich diversity of crystal structures have been prepared within this system. This has been done frequently in the presence of organic template species (amines in most cases).[3] Among these zincophosphates are 3D compounds with extra-large 20- and 24-membered ring channel systems.[4,5] After a first report by Kniep *et al.*,[6] many efforts have also been directed to the synthesis of metallo-borophosphates, and zeotype phases have been discovered recently.[7] However, up to now only a very limited number of 2D and 3D metallo-borophosphates have been prepared successfully using organic template species.[8]

We have now found that a synthesis designed for a framework zinco-borophosphate using 1,6-diaminohexane as a template yielded a layered zincophosphate that, remarkably, contains within the interlayer regions, besides diprotonated diamine units, orthoboric acid molecules. Here, we report the hydrothermal synthesis, a single-crystal X-ray structure analysis, and a combined thermogravimetric (TG), difference thermal analysis (DTA), variable-temperature powder X-ray diffraction (XRD), and FT-IR spectroscopy study of the new compound **I**.

Experimental

Syntheses

In typical syntheses of **I**, 1.76 g boric acid, 6.71 g phosphoric acid (85 wt%), 5.00 g deionized water, 3.25 g 1,6-diaminohexane, and 2.31 g zinc oxide were combined unter stirring. The hydrogels (pH 1–2) were transferred to Teflon-lined stainless steel autoclaves of 8 ml volume (degree of filling 80–95%) and heated at 450 K under static conditions and autogenous pressure for periods between 2.5 and 5.0 days. The white solid products were filtered off in a vaccum, washed successively with water and ethanol, and air-dried at 380 K. Tiny needle-shaped crystals, some of which had a length of up to 0.4 mm, were obtained. Yields were 90% on the basis of zinc oxide. CHN analysis (calc.): C, 11.35 (10.88); H, 3.27 (3.34); N, 3.91 (4.23).

The hydrothermal treatment at 450 K of gels containing both acids, the zinc source and the amine in the stoichiometry given by **I** did not yield solid materials, *i.e.* the synthesis of **I** needs amine and boric acid in excess.

A crystalline dehydrated product of **I** has been identified by TG/XRD measurements (see below). This phase was prepared by heating a sample of **I** in an oven at 510 K for 10 hours. The experimental weight loss of 2.7% indicates the release of one water molecule per formula unit from **I** (calc. weight loss: 2.7%). CHN analysis of the dehydrated product ($C_6H_{20}BN_2O_{14}P_3Zn_3$) (calc.): C, 11.28 (11.19); H, 3.24 (3.13); N, 3.85 (4.35). The material obtained had a very slightly yellow-brownish colour, possibly due to minor degradation of the amine.

Methods of characterization

Thermogravimetric measurements (TG/DTA) were performed on a Netzsch STA 429 analyzer. Samples of **I** of *ca.* 25 mg weight were placed in alumina crucibles and heated in a flowing oxygen atmosphere from room temperature up to 1273 K at a rate of 5 K min^{-1}.

Powder XRD patterns of **I** and the dehydrated product were recorded at room temperature from flat samples in transmission mode on a Guinier-type instrument with image foil detector (Huber G670) using Cu $K\alpha_1$ radiation. Silicon was used as an external standard for 2Θ-calibration.

Variable-temperature powder XRD photographs of **I** were taken on a Guinier camera using Cu $K\alpha_1$ radiation. For this measurement, a powdered sample was filled into a quartz-glass

†Electronic supplementary information (ESI) available: powder XRD data for **I**. See http://www.rsc.org/suppdata/jm/b1/b105057p/

capillary of 0.5 mm diameter (which was left unsealed) and heated in an air atmosphere from room temperature up to 1173 K at a rate of 0.3 K min^{-1}.

FT-IR spectra were recorded between 400 and 4000 cm^{-1} using KBr pellets containing **I** or the dehydrated product on a BioRad Digilab Division FTS-60 spectrometer.

Single-crystal X-ray structure analysis

A needle-shaped crystal of **I**, 0.36 × 0.04 × 0.02 mm^3 in size, was glued to the tip of a glass fibre. All X-ray measurements were done on an Enraf-Nonius CAD4 diffractometer at room temperature using graphite-monochromatized Mo Kα radiation. Empirical absorption corrections on the basis of ψ-scans were applied. For structure solution and refinement the SHELXS97 and SHELXL97 program systems were used.[9] H atoms of methylene groups were geometrically constructed and treated riding on the respective C atom. The coordinates of all H atoms of the NH_3 groups and the boric acid molecule were located on Fourier difference maps and refined independently (with fixed U values). The H atom of the terminal P–OH group (bonded to the O8 atom) could not be determined. Crystal data and further information about the structure determination are collected in Table 1. Final atomic parameters are listed in Table 2.

CCDC reference number 166084. See http://www.rsc.org/suppdata/jm/b1/b105057p/ for crystallographic data in CIF or other electronic format.

Results

Compound **I** has been synthesized under mild hydrothermal conditions from hydrogels of composition $ZnO : P_2O_5 : B_2O_3 : H_2O$: 1,6-diaminohexane = 2 : 2 : 1 : 33 : 2.

Crystal structure

In the structure alternation occurs along the crystallographic a axis with anionic zincophosphate layers (denoted A) and cationic composite layers (denoted a) formed by diprotonated 1,6-diaminohexane and orthoboric acid molecules (Fig. 1) occurring in the sequence AaAa.

The purely inorganic layers are composed of corner-linked ZnO_4, PO_4 and $PO_3(OH)$ tetrahedra with typical values for bond lengths and angles: av. (Zn–O) = 1.948 Å, av. (P–O) = 1.538 Å, av. (Zn–O–P) = 133.1° for 2-coordinated oxygen, av. (Zn–O–P) = 119.0° for 3-coordinated oxygen. Small cage-like building units assembled from five ZnO_4, three PO_4 and one $PO_3(OH)$ tetrahedra may be identified. Such a Zn_5P_4 cage-like unit is shown in Fig. 2. It possesses one ring formed by three tetrahedra (which is therefore denoted a 3-membered ring), four 4-membered rings and one 5-membered ring. It can be seen that one of the unique oxygen atoms, O(1), is 3-coordinated [P–(μ_3-O)–Zn_2 bridge]. All other unique oxygen atoms are 2-coordinated [Zn–O–P bridges] with the exception of the O(8) atom, which is attached only to a phosphorus atom. However, a bond-valence sum calculation[10] clearly suggests that the O(8) atom is part of a terminal P–OH

Table 1 Crystal data and details of structure analysis for $[Zn_3(PO_4)_2(HPO_4)]\cdot H_3N(CH_2)_6NH_3\cdot B(OH)_3$ (**I**)

Empirical formula	$C_6H_{22}BN_2O_{15}P_3Zn_3$
Formula weight	662.08
Crystal system	Monoclinic
Space group; Z	$P2_1/c$; 4
a/Å	12.955(1)
b/Å	8.295(1)
c/Å	18.805(2)
β/°	91.34(1)
V/$Å^3$	2020.3(4)
T/K	293
μ/mm^{-1}	3.846
ρ_{calc}/mg mm^{-3}	2.177
Reflections measured	5092
Unique reflections (total); R_{int}	4885; 0.049
Unique reflections ($I > 2\sigma_I$)	2712
Parameters refined	298
$R1^a$ ($I > 2\sigma_I$)	0.052
$wR2^b$ (all data)	0.097
Largest diff. peak, hole/e $Å^3$	+0.79, −0.81

$^a R1 = \Sigma(|F_{obs}| - |F_{calc}|)/\Sigma|F_{obs}|$. $^b wR2 = [\Sigma[w(F^2_{obs} - F^2_{calc})^2]/\Sigma[w(F^2_{obs})^2]]^{0.5}$.

Table 2 Final refined coordinates and equivalent isotropic displacement parameters ($Å^3$) for $[Zn_3(PO_4)_2(HPO_4)]\cdot H_3N(CH_2)_6NH_3\cdot B(OH)_3$ (**I**)

Atom	x	y	z	$U_{eq}{}^a/U_{iso}$
Zn(1)	0.89594(6)	0.8595(1)	0.19334(4)	0.0149(2)
Zn(2)	0.88265(6)	0.95977(9)	0.27816(4)	0.0157(2)
Zn(3)	0.88265(6)	0.95977(9)	0.41356(4)	0.0137(2)
P(1)	0.9464(1)	0.6451(2)	0.32172(8)	0.0124(3)
P(2)	0.1155(1)	0.0745(2)	0.41751(8)	0.0123(4)
P(3)	0.2622(1)	0.5740(2)	0.21492(8)	0.0150(4)
O(1)	0.9941(3)	0.7588(5)	0.2640(2)	0.017(1)
O(2)	0.9017(3)	0.7426(5)	0.3822(2)	0.019(1)
O(3)	0.9680(3)	1.0345(5)	0.1483(2)	0.018(1)
O(4)	0.0005(3)	0.1073(5)	0.4271(2)	0.017(1)
O(5)	0.8276(3)	0.9392(5)	0.5095(2)	0.015(1)
O(6)	0.1335(3)	0.9151(5)	0.3782(2)	0.018(1)
O(7)	0.8603(3)	0.5467(6)	0.2846(2)	0.018(1)
O(8)	0.3830(3)	0.5376(6)	0.2098(2)	0.026(1)
O(9)	0.1653(3)	0.2139(5)	0.3760(2)	0.016(1)
O(10)	0.2199(4)	0.5829(6)	0.1395(2)	0.028(1)
O(11)	0.2226(4)	0.4299(6)	0.2558(2)	0.026(1)
O(12)	0.2511(4)	0.7307(6)	0.2548(2)	0.026(1)
O(13)	0.3640(4)	0.1520(9)	0.3591(3)	0.034(1)
O(14)	0.3776(4)	0.0676(8)	0.4821(3)	0.034(1)
O(15)	0.5238(4)	0.0896(8)	0.4105(3)	0.037(2)
B	0.4189(6)	0.104(1)	0.4176(4)	0.023(2)
H(1)	0.316(6)	0.05(1)	0.484(4)	0.05
H(2)	0.315(6)	0.15(1)	0.364(5)	0.05
H(3)	0.549(7)	0.07(1)	0.443(4)	0.05
N(1)	0.1098(5)	0.6768(8)	0.4835(3)	0.025(1)
H(11)	0.077(7)	0.63(1)	0.457(4)	0.05
H(12)	0.133(6)	0.76(1)	0.453(4)	0.05
H(13)	0.057(6)	0.72(1)	0.508(4)	0.05
N(2)	0.6564(5)	0.655(1)	0.2901(4)	0.036(2)
H(21)	0.750(6)	0.623(9)	0.284(4)	0.05
H(22)	0.633(6)	0.68(1)	0.246(4)	0.05
H(23)	0.662(7)	0.75(1)	0.307(4)	0.05
C(1)	0.1892(6)	0.592(1)	0.5267(4)	0.031(2)
C(2)	0.2719(5)	0.5145(9)	0.4810(4)	0.031(2)
C(3)	0.3444(6)	0.631(1)	0.4444(4)	0.035(2)
C(4)	0.4267(5)	0.541(1)	0.4032(4)	0.030(2)
C(5)	0.5023(6)	0.649(1)	0.3665(4)	0.036(2)
C(6)	0.5842(6)	0.553(1)	0.3310(4)	0.036(2)

$^a U_{eq}$ is defined as one third of the trace of the orthogonalized U_{ij} tensor.

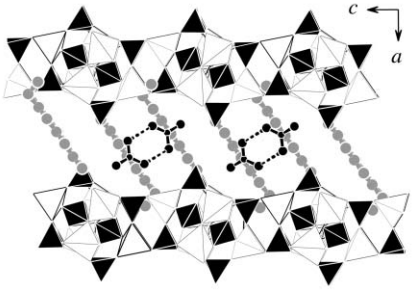

Fig. 1 The layered structure of $[Zn_3(PO_4)_2(HPO_4)]\cdot H_3N(CH_2)_6NH_3\cdot H_3BO_3$ (**I**) as viewed down the b axis. Zincophosphate layers are represented as corner-sharing ZnO_4 (white) and $PO_4/PO_3(OH)$ tetrahedra (black). Gray spheres represent C and N atoms of organic dications. Black spheres represent B and O atoms of boric acid dimers, the hydrogen bonds of which are indicated by dashed lines.

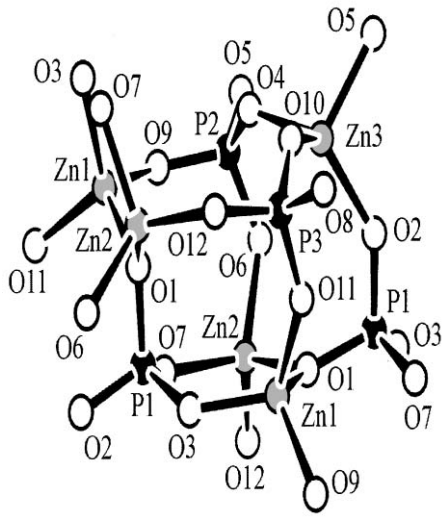

Fig. 2 A Zn_5P_4 cage-like unit in **I**.

group. By sharing all atoms of O(1)-centered PZn_2 triangles [P–(μ_3-O)–Zn_2 bridges], the cage-like units are organized into columns of 2_1-symmetry running along the *b* axis (Fig. 3). Each column is further linked to two adjacent ones by Zn–O–P bridges forming 4-membered rings. In this way, an inorganic layer is generated, which possesses large 8-membered ring windows in an approximately hexagonal array.

In their bilayer-like arrangement, the organic dications are inclined with their long molecular axes against the normals of the planar zincophosphate layers (Fig. 1) and are located near the 8-membered ring windows. The conformation of each dication is *anti* around all C–C bonds with one exception. Around the C(1)–C(2) bond a *gauche* conformation is found which serves to orient the corresponding NH_3 group [N(1) atom] into a large window. The dications interact quite strongly by two- and three-centre[11] N–H···O hydrogen bonds with the adjacent inorganic layers and also with boric acid molecules. Geometrical parameters for the hydrogen bonds are collected in Table 3. This table also lists the parameters of some C–H···O contacts, which may be considered as very weak hydrogen bonds.[12]

The trigonal planar boric acid molecules form centrosymmetric dimers (Fig. 4) by strong hydrogen-bonding interactions (Table 3), which, in turn, link two adjacent zincophosphate layers at the positions where 4-membered rings connect the columns. The pattern that results from the 2D packing of both

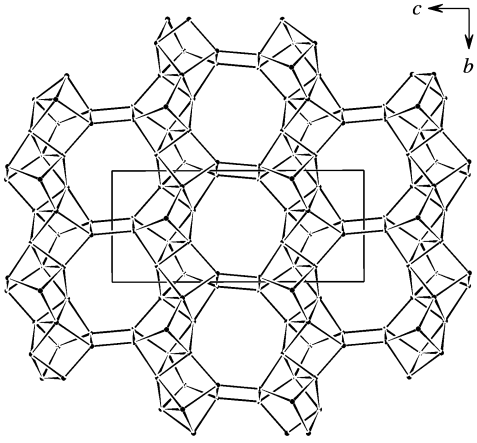

Fig. 3 The topology of a zincophosphate layer in **I** as viewed down the *a* axis. Only the connectivities between the Zn and P atoms are shown. Columns constructed from Zn_5P_4 cage-like units extend parallel to the *b* axis.

Table 3 Hydrogen bonds for $[Zn_3(PO_4)_2(HPO_4)]\cdot H_3N(CH_2)_6NH_3\cdot B(OH)_3$ (**I**)

Moiety	D–H	H···A	D···A	D–H···A
O(8)–H*···O(15)[a]			2.629(7)	
O(14)–H(1)···O(5)[b]	0.81(8)	1.87(8)	2.666(6)	169(9)
O(13)–H(2)···O(9)	0.64(8)	2.02(8)	2.651(7)	165(13)
O(15)–H(3)···O(14)[c]	0.71(8)	2.02(8)	2.700(8)	160(10)
N(1)–H(11)···O(3)[d]	0.77(9)	2.19(8)	2.904(7)	155(8)
N(1)–H(12)···O(6)	0.93(8)	1.92(8)	2.820(7)	160(7)
N(1)–H(13)···O(4)[e]	0.92(8)	2.02(8)	2.861(7)	152(7)
N(2)–H(21)···O(7)	1.22(8)	1.59(8)	2.793(9)	167(6)
N(2)–H(22)···O(13)[a]	0.92(8)	1.97(8)	2.812(9)	151(7)
N(2)–H(23)···O(8)[a]	0.88(9)	2.45(9)	3.22(1)	146(7)
N(2)–H(23)···O(11)[a]	0.88(9)	2.42(9)	2.911(9)	116(6)
C(1)–H(1A)···O(2)[b]	0.99	2.50	3.480(9)	169
C(1)–H(1B)···O(10)[f]	0.99	2.54	3.450(9)	152
C(2)–H(2B)···O(9)	0.99	2.49	3.449(9)	163
C(4)–H(4B)···O(13)	0.99	2.68	3.423(9)	132

Atom H* not determined. Symmetry transformations:[a] $-x+1$, $y+0.5$, $-z+0.5$; [b] $-x+1$, $-y+1$, $-z+1$; [c] $-x+1$, $-y$, $-z+1$; [d] $-x+1$, $y-0.5$, $-z+0.5$; [e] $-x$, $-y+1$, $-z+1$; [f] x, $-y+1.5$, $z+0.5$.

dications and boric acid molecules within a composite layer when viewed down the *a* axis is illustrated in Fig. 5. This pattern, the molecular information of which is transcribed onto the zincophosphate layers *via* the hydrogen-bonding interactions, may be described on the basis of two planar, slightly distorted 3^6 nets. These nets are formed by pairs of dications (related by an inversion centre) and hydrogen-bonded boric acid dimers, respectively. Both 3^6 nets interpenetrate each other in such a way that all nodes of one net sit on the midpoints of the shortest links of the other net. On its side

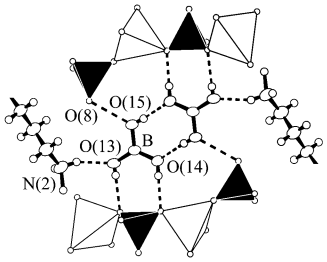

Fig. 4 The local environment of a centrosymmetric boric acid dimer in **I**. White and black tetrahedra are centered by Zn and P atoms, respectively. Dashed lines represent hydrogen bonds. The H atom attached to the O(8) atom in the O(8)···O(15) hydrogen bond has not been determined.

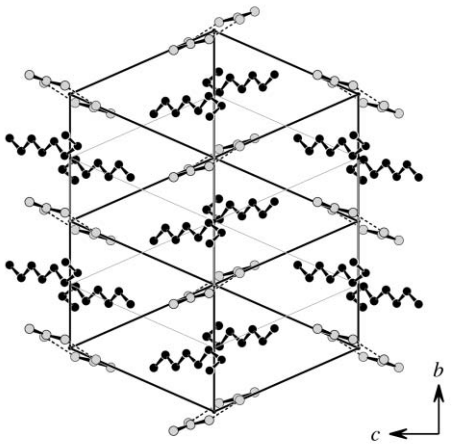

Fig. 5 Array of organic dications (black spheres) and boric acid dimers (gray spheres) in a composite layer of **I** as viewed down the *a* axis.

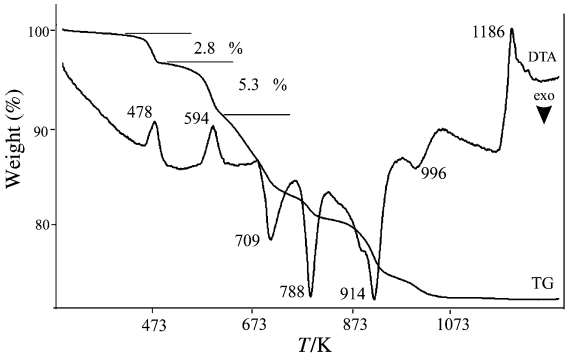

Fig. 6 TG/DTA curves of **I** (flowing oxygen atmosphere).

surfaces, each boric acid molecule interacts by van der Waals forces with methylene group atoms (Fig. 1).

Thermal behaviour

The TG/DTA curves of **I** (Fig. 6) in connection with a variable-temperature powder XRD photograph (not shown) may be interpreted as follows: During the first endothermic event between 426 and 499 K, **I** transforms with the release of one water molecule (calc. weight loss 2.7%) into a new crystalline phase. From this dehydrated product approximately two further water molecules are released during the second endothermic event between 499 and 615 K and the material becomes amorphous at *ca.* 600 K. Thereafter, the amine is oxidatively decomposed in a series of steps (exothermic events) until 1073 K. In the course of decomposition, as yet unidentified material crystallizes at *ca.* 895 K. At temperatures higher than *ca.* 1090 K, the crystalline material is essentially β-$Zn_2P_2O_7$ (PDF: 34-1275). The total weight loss of 26.3% agrees with the loss of amine and water originating from boric acid and P–OH groups (calc. 25.7%).

The experimental room-temperature XRD patterns of **I** and the crystalline dehydrated product are compared in Fig. 7. Fig. 7 also includes an XRD pattern simulated using the crystal-structure data of **I**. The phase purity of **I** is demonstrated by the good agreement of the diffractograms. Additionally, the following cell parameters were obtained by a least-squares fit of the experimental diffraction lines of **I** using *hkl* indices from the single-crystal work: $a = 12.959(8)$, $b = 8.286(4)$, $c = 18.84(1)$ Å, $\beta = 91.30(5)^\circ$. The cell parameters are in agreement with those determined by single-crystal XRD. No attempt has been made to determine the structure of the dehydrated product from the low-resolution powder XRD data. However, the diffractograms indicate that

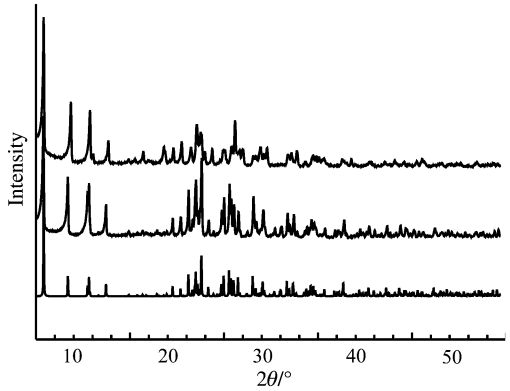

Fig. 7 Powder XRD patterns (Cu $K\alpha_1$ radiation): **I**, simulated from crystal structure data (bottom); **I**, experimental (middle); dehydrated product, experimental (top).

the dehydrated product is structurally closely related to **I**, and is likely to contain the same zincophosphate layers.

The release of one water per formula unit from **I** as measured by TG suggests from stoichiometry and structural arguments that condensation takes place between the terminal P–OH groups and boric acid molecules, but not between boric acid. Probably, the P–O(8)–H···O(15)–B hydrogen bonds are transformed into P–O–B bridges and the O(15)–H(15)···O(14) hydrogen bonds connecting boric acid molecules, which are the longest O–H···O bonds in **I**, are also broken (see Fig. 4). Such a reaction scheme is supported by the differences in the IR spectra. A band at 1261 cm^{-1} [in-plane (P)–O–H···O bending modes[13]] and two bands at 884 and 874 cm^{-1} [out-of-plane (P)–O–H···O bending modes[13]] appear in the spectrum of **I** but not in that of the dehydrated product. In the spectrum of the latter compound, on the other hand, a band is seen at 1354 cm^{-1}, which is absent in the spectrum of **I** and which we tentatively assign to B–O–P stretching modes involving trigonally coordinated boron.[14]

Discussion

The most interesting aspect of the formation of **I** is the role of boric acid, *i.e.* its function as a template together with the organic dications, to lead to a layered metallophosphate. Such co-templating of H_3BO_3 has not been reported before. That such co-templating may lead to new materials has been demonstrated recently for some aluminophosphates by using mixtures of amines.[15] Indeed, the structural elements existing in **I**, *i.e.* columns of Zn_5P_4 cage-like units linked *via* 4-membered rings into layers, have only very recently been found in two other zincophosphates containing protonated triethylenetetramine molecules, $[Zn_6(PO_4)_4(HPO_4)_2]C_6H_{22}N_4$,[16] and tris-(2-aminoethyl)amine molecules, $[Zn_6(PO_4)_4(HPO_4)_2]\cdot C_6H_{21}N_4\cdot NH_4\cdot H_2O$.[17] Stereochemically different linkages of columns results in puckered layers (*cis* linkage) in the former compound (see Fig. 5 in ref. 16) and nearly planar layers (*trans* linkage) in the latter compound and in **I** (Fig. 1). The other two zincophosphates which have been prepared in the presence of 1,6-diaminohexane molecules possess 2D and 3D framework structures that are completely different from the structure of **I**.[4,18] Interestingly, in 2D $[Zn_3(HPO_4)_4]\cdot H_3N(CH_2)_6NH_3\cdot H_2O$ the diprotonated amine molecules are oriented with their long molecular axis parallel to the inorganic layers. This contrasts with the bilayer-like arrangement of the dications in **I** that is obviously stabilized by the boric acid molecules.

It is also interesting to notice that the incorporation of boron species into metallophosphate frameworks by hydrothermal methods using various organic templates has been repeatedly reported to be unsuccessful.[5,19] The reasons for this are not clear yet, since the mechanisms of formation of organically-templated open-framework materials are only poorly understood. In this context, the structure of **I** may be of interest because it points to an important molecular property of H_3BO_3, namely its "hydrophilic/hydrophobic" character. This may be considered in further synthesis design of metalloborophosphates, *e.g.* by use of solvothermal methods.

Acknowledgement

I thank Professor J. Felsche for providing the laboratory and intrumental equipment and A. Straub and G. Wildermuth for technical assistance.

References

1 A. K. Cheetham, G. Ferey and T. Loiseau, *Angew. Chem., Int. Ed.*, 1999, **38**, 3268.
2 T. E. Gier and G. D. Stucky, *Nature*, 1991, **349**, 508;

W. T. A. Harrison, T. E. Gier, K. L. Moran, J. M. Nicol, H. Eckert and G. D. Stucky, *Chem. Mater.*, 1991, **3**, 27.
3 A. Choudhury, S. Neeraj, S. Natarajan and C. N. R. Rao, *J. Mater. Chem.*, 2001, **11**, 1537; C. N. R. Rao, S. Natarajan, A. Choudhury, S. Neeraj and R. Vaidhyanathan, *Acta Crystallogr., Sect. B*, 2001, **57**, 1; C. N. R. Rao, S. Natarajan, A. Choudhury, S. Neeraj and A. A. Ayi, *Acc. Chem. Res.*, 2001, **34**, 80; W. T. A. Harrison, *Int. J. Inorg. Mater.*, 2001, **3**, 179; P. Zhang, Y. Wang, G. Zhu, Z. Shi, Y. Liu, H. Yuan and W. Pang, *J. Solid State Chem.*, 2000, **154**, 368; A. A. Ayi, A. Choudhury, S. Natarajan and C. N. R. Rao, *J. Mater. Chem.*, 2000, **10**, 2606; W. Liu, Y. Liu, Z. Shi and W. Pang, *J. Mater. Chem.*, 2000, **10**, 1451; S. Neeraj and S. Natarajan, *Chem. Mater.*, 2000, **12**, 2753 and references therein.
4 J. A. Rodgers and W. T. A. Harrison, *J. Mater. Chem.*, 2000, **10**, 2853.
5 G.-Y. Yang and S. C. Sevov, *J. Am. Chem. Soc.*, 1999, **121**, 8389.
6 R. Kniep, G. Götzel, B. Eisenmann, C. Röhr, M. Asbrand and M. Kizilyalli, *Angew. Chem., Int. Ed. Engl.*, 1994, **34**, 749.
7 I. Boy, F. Stowasser, G. Schäfer and R. Kniep, *Chem. Eur. J.*, 2001, **7**, 834; A. Yilmanz, X. Bu, M. Kizilyalli and G. D. Stucky, *Chem. Mater.*, 2000, **12**, 3243; G. Schäfer, H. Borrmann and R. Kniep, *Microporous Mesoporous Mater.*, 2000, **41**, 161 and references therein.
8 G. Schäfer, H. Borrmann and R. Kniep, *Z. Anorg. Allg. Chem.*, 2001, **627**, 61; R. Kniep and G. Schäfer, *Z. Anorg. Allg. Chem.*, 2000, **626**, 141; R. P. Bontchev, J. Do and A. J. Jacobson, *Inorg. Chem.*, 2000, **39**, 3320 and references therein.
9 G. M. Sheldrick, SHELXS97 and SHELXL97, University of Göttingen, Germany, 1997.
10 I. D. Brown and D. Altermatt, *Acta Crystallogr., Sect. B*, 1985, **41**, 244.
11 G. A. Jeffrey and W. Saenger, *Hydrogen Bonding in Biological Structures*, Springer, Berlin, 1994, p. 35.
12 T. Steiner and G. Desiraju, *Chem. Commun.*, 1998, 891.
13 J. Emsley and D. Hall, *The Chemistry of Phosphorus*, Harper & Row, London, 1976, p. 102.
14 A. Bertoluzza, P. Monti, M. A. Battaglia and S. Bonora, *J. Mol. Struct.*, 1980, **64**, 123.
15 A. M. Chippindale, S. Natarajan, J. M. Thomas and R. H. Jones, *J. Solid State Chem.*, 1994, **111**, 18; R. H. Jones, A. M. Chippindale, S. Natarajan and J. M. Thomas, *Chem. Commun.*, 1994, 565; S. Oliver, A. Kuperman, A. Lough and G. A. Ozin, *Inorg. Chem.*, 1996, **35**, 6373; J. Li, J. Yu, W. Yan, Y. Xu, W. Xu, S. Qiu and R. Xu, *Chem. Mater.*, 1999, **11**, 2600.
16 A. Choudhury, S. Natarajan and C. N. R. Rao, *J. Solid State Chem.*, 2001, **157**, 110.
17 A. A. Ayi, A. Choudhury, S. Natarajan, S. Neeraj and C. N. R. Rao, *J. Mater. Chem.*, 2001, **11**, 1181.
18 D. Chidambaram, S. Neeraj, S. Natarajan and C. N. R. Rao, *J. Solid State Chem.*, 1999, **147**, 154.
19 S. Ekambaram, C. Serre, G. Ferey and S. C. Sevov, *Chem. Mater.*, 2000, **2**, 444; S. Ekambaram and S. C. Sevov, *Angew. Chem. Int. Ed.*, 1999, **38**, 372; S. B. Harmon and S. C. Sevov, *Chem. Mater.*, 1998, **10**, 3020.